INTERNATIONAL ATOMIC ENERGY AGENCY
UNITED NATIONS EDUCATIONAL, SCIENTIFIC AND CULTURAL ORGANIZATION
INTERNATIONAL CENTRE FOR THEORETICAL PHYSICS
I.C.T.P., P.O. BOX 586, 34100 TRIESTE, ITALY, CABLE CENTRATOM TRIESTE

SMR/406-4

THIRD AUTUMN WORKSHOP ON ATMOSPHERIC
RADIATION AND CLOUD PHYSICS
27 November - 15 December 1989

"Clouds and Radiation"

Marcia BAKER
University of Washington
Department of Geophysics
Seattle, WA
USA

Please note: These are preliminary notes intended for internal distribution only.

Clouds and Radiation

I. Background

A. Solar and Terrestrial Radiation

It is convenient to discuss atmospheric radiation, and in particular, the interactions of atmospheric radiation with clouds, under two separate headings, according to the origin of the radiation (the Sun or the Earth). The temperature of the radiation source determines its spectrum. Figure 1.1a shows the normalised energy spectrum of radiation $B_\lambda(T)$ (Watts/m^2/steradian) emitted from a black body at temperature T=5750 K, which is near the radiative temperature of the sun, and that of a black body at T=245 K, approximately the radiative temperature of the atmosphere. The areas under the curves are proportional to the total power per area from each body at the top of the atmosphere; that from the sun is reduced greatly because of the distance between the Earth and the Sun. The function $B_\lambda(T)$ is

$$B_\lambda(T) = \frac{hc}{\lambda^3}\cdot\frac{1}{(\exp^{\frac{hc}{k\lambda T}}-1)}$$

where $h \approx 6.6\times10^{-34} Js$ is Planck's constant, $c = 3x10^8 ms^{-1}$ is the speed of light, and $k = 1.38x10^{-23} J^\circ\ molecule^{-1}$ is Boltzmann's constant. From this expression we can derive Wien's Law, which gives the wavelength at which radiation from a black body at temperature T is maximum:

$$\lambda_{MAX}(\mu) \approx \frac{2900}{T}(K) \qquad (1.1)$$

The solar radiation is called shortwave (SW) because the spectrum peaks at a wavelength $\lambda_{MAX} \approx 0.5$ microns and there is almost no energy in the solar beam at wavelengths $\lambda \geq 5$ microns. The intensity of solar radiation vertically incident at the top of our atmosphere is $S_o = 1380 Wm^{-2}$, where S_o is called the solar constant. The total annually and diurnally averaged solar flux (power per area) at the top of our atmosphere is

$$\frac{S_o \cdot \pi R_E^2}{4\pi R_E^2} \equiv \frac{S_o}{4}$$

$=345 Watts/m^2$ = the total flux of outgoing terrestrial radiation in equilibrium. The terrestrial (sometimes called longwave, or LW) radiation spectrum peaks at $\lambda \approx 10$ microns.

The wavelength regimes in which solar and terrestrial radiation are important are:

$$\left.\begin{array}{l} 0.01\text{–}0.1\ \mu\ x\text{–}ray \\ 0.1\text{–}0.8\ \mu\ visible \end{array}\right\} solar$$

$$\left.\begin{array}{l} 0.8\text{–}10.0\ \mu\ near\ infrared\ (IR) \\ 10.0\text{–}100\ \mu\ far\ infrared \end{array}\right\} terrestrial$$

The topic of the next few lectures is the interaction of the solar and terrestrial radiation with atmospheric water clouds, as shown schematically in Figure 1.2. We will consider clouds to be horizontally infinite, homogeneous sheets of finite thickness which absorb and scatter both SW and LW radiation. (The subjects of inhomogeneous, finite, and glaciated clouds will be treated later.)

The interactions of clouds with radiation have two major effects. First, the radiative fluxes are modified by scattering from and passage through clouds, which leads to direct modifications in global and local heat budgets. Second, the clouds themselves are modified by the same process, which has indirect impacts on the heat budgets. We will discuss both effects briefly here.

B. Interactions of Photons with Gases and Particles

Given the fluxes of SW and LW radiation impinging on a horizontal cloud layer of known properties, we wish to calculate, or estimate the fluxes inside the clouds, the rate of energy absorption by the clouds, and the flux of energy reflected by them.

The energy removed from the beam in traversing a horizontal cloud layer may be (a) absorbed by atoms and molecules and then re-emitted at a different wavelength, (b) absorbed by atoms, molecules, drops and small particles and transformed into heat, raising the local temperature in the medium, and/or (c) simply redirected, or scattered by molecules, small particles and drops.

Figure 1.1b shows the fraction of electromagnetic energy absorbed by the atmosphere as a function of wavelength λ. Molecular absorption is wavelength dependent because molecules possess discrete energy levels associated with different vibrational and rotational states. Absorption of a photon can only occur if the photon has exactly enough energy to raise the molecule from one of its discrete states to another. The energy of a photon is a function of its wavelength λ, or its frequency $\upsilon = \frac{c}{\lambda}$ (where $c = 3\times10^8 \frac{m}{s}$ is the velocity of light). Therefore photons of only one discrete value of λ can be absorbed in any transition. However, in general, the vibrational-rotation transitions correspond to energies that are grouped in bands. Moreover, collisions of molecules and/or their motion and other temperature and pressure effects cause broadening of the range of possible photon wavelengths that can be absorbed. Therefore, calculation of the absorptivity of the atmosphere as a function of wavelength is accordingly extremely complex.

The interactions of radiative fluxes and small droplets depend on the wavelength of the radiation and the size of the droplets. To understand this dependence physically, consider a plane wave of wavelength λ incident on a sphere of radius a and index of refraction m as shown in Figure 1.3. The radiation will in part pass through the sphere, and be refracted by it, and in part it will be diffracted around its surface. The amount of energy scattered away from the forward direction, and the amount of energy removed (absorbed) by the interaction depends on the interference between the forward propagating wave and the refracted and diffracted waves. The interference in turn depends on the phase change $\Delta\gamma$ suffered by the photons passing through the sphere, which is on the order of

$$\Delta\gamma = 4\frac{\pi}{\lambda}\cdot a(m-1) \qquad (1.2)$$

In general, we will see that we need consider scattering only by particles of spatial dimension a such that

$$\Delta\gamma \geq 4$$

The index of refraction of water = $m \approx 1.33$ and a typical drop size in low-level clouds is $a \approx 5$ μm. Thus, since $\Delta\gamma \approx \frac{4\pi}{10}\cdot 5\ (.33) \approx 2$, we can ignore scattering of LW radiation by most cloud drops. For rough estimates of the radiative fluxes we can also ignore scattering of both LW and SW radiation by atoms and molecules, to first approximation. (See Slingo and Schrecker, 1982, and Roach and Slingo, 1979, and references therein for more complete treatments.)

We now consider the passage of LW and then SW radiation through a homogeneous cloud.

C. The One-Dimensional Equations of Radiative Transfer

In this section we will derive the equations of radiative transfer in one dimension. The equations depend on certain parameters that describe the medium, which for the moment we suppose are known. In section II we discuss these parameters and simple approximations for them.

1. Background. Consider a horizontal slab of material of density ρ (kg/m^3) and thickness dz, and a beam of radiation of wavelength λ and intensity, or radiance, I_λ (*Watts/m^2/steradian*) incident vertically on it. Lambert's Law states that the intensity removed from the beam in traversing a distance dz by absorption is

$$dI_\lambda = -I_\lambda \kappa_\lambda^{abs} \rho dz$$

where $\kappa_\lambda^{abs}(\frac{m^2}{kg})$ is the absorption coefficient, a constant depending on the medium. If the radiation is LW, it

will excite molecular transitions that will result in the reemission of energy in other wavelengths, thus increasing I_λ again. If we are dealing with SW radiation, we must consider scattering, which is responsible both for part of the decrease in I_λ, and then, as radiation is scattered back into the forward travelling beam, for its increase. We consider each of these cases separately.

2. LW Radiation. Let equation (1.2) represent the decrease in energy due to absorption by molecules from a beam of LW radiation travelling vertically upward, as in Figure 1.4a. We ignore scattering, as mentioned above, but we must consider reemission of the absorbed radiation. Kirchoff's Law tells us energy will be re-emitted uniformly in all directions, spread over all wavelengths with a spectrum proportional to $\kappa_\lambda^{abs} B_\lambda(T)$, where T is the temperature of the slab and $B_\lambda(T)$ is the black body function shown in Figure 1.1a. Thus the total change in $I_\lambda^\uparrow$ crossing dz is

$$dI_\lambda^\uparrow = -\kappa_\lambda^{abs}\rho I_\lambda^\uparrow dz + \kappa_\lambda^{abs} B_\lambda \rho dz \tag{1.3}$$

Equation (1.3) (and its counterpart, for radiation travelling downward) applies only to radiation travelling vertically, whereas in reality radiation is travelling in all directions. To reduce the problem to one dimension, we integrate the intensities over the upward and downward hemispheres to define

$$\int_{-\frac{\pi}{2}}^{\frac{\pi}{2}} 2\pi I_\lambda(\theta)\cos\theta\sin\theta d\theta \equiv F_\lambda^\uparrow \tag{1.4}$$

$$\int_{\frac{\pi}{2}}^{-\frac{\pi}{2}} 2\pi I_\lambda(\theta)\cos\theta\sin\theta d\theta \equiv F_\lambda^\downarrow$$

where F are the functions called irradiances, or fluxes. They represent the total energy crossing unit horizontal area per unit time (see Figure 1.4b). We shall concern ourselves here only with the calculation of the fluxes, $F^\uparrow$ and $F^\downarrow$. It can be shown that equation (1.3) holds to a very good approximation with I_λ replaced by F_λ, if we replace dz by a mean thickness $\frac{5}{3}dz$ and we replace $B_\lambda(T)$ by its value integrated over a hemisphere, which is $\pi B_\lambda(T) = \sigma T^4$, where $\sigma = 5.8 \times 10^{-8}\ W/m^2/K^4$ is the Stefan-Boltzmann constant. We define the optical depth

$$\tau_\lambda^{abs}(z) = \frac{5}{3}\int_z^\infty \kappa_\lambda^{ext}\rho dz \tag{1.5}$$

with $\tau = 0$ at the top of the atmosphere, and $\tau = \tau^*$ at the Earth's surface, as in Figure 1.4. Then we have from the flux version of equation (1.3) and its counterpart for downward propagating radiation that

$$\frac{dF_\lambda^\uparrow}{d\tau_\lambda} = F_\lambda^\uparrow - \pi B_\lambda(T) \tag{1.6a}$$

$$\frac{dF_\lambda^\downarrow}{d\tau_\lambda} = -F_\lambda^\downarrow + \pi B_\lambda(T) \tag{1.6b}$$

(Note that these equations are identical to those presented in, for example, Roach and Slingo, 1979, in different notation.) Furthermore, the absorption of energy by the slab changes its temperature. The net rate of energy absorption (Watts/m^3) at height z is

$$\frac{d}{dz}\int(F_\lambda^\downarrow(z) - F_\lambda^\uparrow(z))d\lambda$$

so the heat equation is

$$\rho c_p \frac{dT(z)}{dt} = \frac{d}{dz}\int(F_\lambda^\downarrow(z) - F_\lambda^\uparrow(z))d\lambda \tag{1.7}$$

Given the initial and boundary conditions for the fluxes and temperature, as well as the function κ_λ^{ext}, the hemispherically averaged LW fluxes and temperature in a uniform nonscattering atmosphere can be found as functions of space and time via equations (1.6) and (1.7). The boundary conditions in the simplest case are: $F_\lambda^\downarrow(0)$ (IR flux at cloudtop) and $F_\lambda^\uparrow(\tau_\lambda^*) = \pi B_\lambda(T_G)$, where T_G is the surface temperature.

We will come back to these equations later, and use them to describe the passage of terrestrial, or LW, infrared radiation through clouds.

3. SW Radiation. We now turn our attention to deriving equations analogous to (1.6) for passage of SW radiation through clouds where we must include scattering because $A\gamma = \frac{12.5}{0.5}(.3) = 40$. In this case we define the scattering and absorption coefficients, $\kappa_\lambda^{scattering}$ and $\kappa_\lambda^{absorption}$ such that

$$\kappa_\lambda^{ext} = \kappa_\lambda^{sc} + \kappa_\lambda^{abs} \tag{1.8}$$

to account for the separate contributions of scattering and absorption to the total extinction of radiation. These depend on the molecules and particles in the medium, as explained in section 1.b. We define the single scattering albedo,

$$\omega_0^\lambda \equiv \frac{\kappa_\lambda^{sc}}{\kappa_\lambda^{sc} + \kappa_\lambda^{abs}} = \frac{(\kappa_\lambda^{ext} - \kappa_\lambda^{abs})}{\kappa_\lambda^{ext}} \tag{1.9}$$

ω_0^λ is the probability a photon of wavelength λ will be scattered (which could mean scattered in the forward direction), rather than absorbed, in any single event. Scattering can redirect photons in any direction, as shown schematically in Figure 1.5. We will continue to consider only one-dimensional radiative transfer, so we are interested only in how much of the scattered radiation is scattered up and how much down. This is usually expressed in terms of "the asymmetry factor" g_λ, where

$$g_\lambda \equiv \frac{2\pi\int_0^\pi \cos\theta I_\lambda^{sc}(\theta)\sin\theta d\theta}{I_\lambda^{incident}} \tag{1.10}$$

$I_\lambda^{sc}(\theta)$ is the intensity of radiation scattered through an angle θ. (We assume azimuthal symmetry). ω_0^λ and g_λ, as well as τ_λ, depend primarily on the numbers and sizes of the cloud drops.

We do not have to consider reemission of radiation, as we did for the LW case (equations 1.3 and 1.6) for the following reason: By Kirchoff's Law a cloud at temperature T emits a spectrum proportional to $\kappa_\lambda^{abs} B_\lambda(T)$. However, (see Figure 1.1a) $B_\lambda(T_{atmosphere})$ is almost zero at solar wavelengths. Thus we can neglect black body emission at solar wavelengths and consider only absorption (by gases and drops) and scattering (by drops).

The most satisfactory one-dimensional approximation to the equations of transfer of solar radiation in water clouds is the so-called delta-Eddington approximation (Joseph et al., 1976), in which the upward fluxes are given in terms of two functions, I_{0_λ} and I_{1_λ} by

$$F_\lambda^\uparrow(\tau_\lambda) = \pi[I_{0_\lambda} + \frac{2}{3}I_{1_\lambda}] \tag{1.11}$$

$$F_\lambda^{\downarrow}(\tau_\lambda) = \pi[I_{0_\lambda} + \frac{2}{3} I_{1_\lambda}] \tag{1.12}$$

where

$$\frac{dI_{0_\lambda}}{d\tau_\lambda} = -(1 - \omega_{0_\lambda} g_\lambda) I_{1_\lambda} + \frac{3}{4}\omega_{0_\lambda} g_\lambda \mu_0 F_{0_\lambda} e^{-\frac{\tau^\lambda}{\mu_0}} \tag{1.13}$$

$$\frac{dI_{1_\lambda}}{d\tau_\lambda} = -3(1 - \omega_{0_\lambda}) I_{0_\lambda} + \frac{3}{4}\omega_{0_\lambda} F_{0_\lambda} e^{-\frac{\tau^\lambda}{\mu_0}} \tag{1.14}$$

F_{0_λ} is the intensity of the direct solar beam at wavelength λ, which is incident at angle $\theta_0 = \cos^{-1}(\mu_0)$. (This is one of a family of approximations of similar form; the choice depends on the particular problem to be solved (Meador and Weaver, 1980).) These equations are solved in terms of initial and boundary conditions on the temperature and fluxes, and the change in layer temperature due to the net absorption of electromagnetic energy is again given by equation (1.7).

Equations (1.13) and (1.14) give the SW radiative fluxes and the temperature inside clouds if the coefficients ω_0^λ, τ^λ, and g_λ are known, as well as the initial and boundary conditions. The boundary conditions are the value of F_0^λ (the intensity in the incident direct beam), that of $\mu_0 = \cos\theta_0$ (the cosine of the solar zenith angle), and A_λ, the albedo of the underlying surface, where

$$F_\lambda^{\uparrow}(\tau_\lambda^*) = \pi A_\lambda F_\lambda^{\downarrow}(\tau_\lambda^*) \tag{1.15}$$

These equations, with equations (1.6) for LW radiation, are the ones we set out to find. We now examine the dependence of the parameters in these equations on the cloud properties.

4. Parameters in the Radiative Transfer Equations. The parameters we need in equations (1.6), (1.7), (1.13), and (1.14) are as follows: Common to all the equations is the optical depth,

$$\tau_\lambda = \int \kappa_\lambda^{ext} \rho dz \tag{1.16a}$$

At short wavelengths τ_λ is a function mainly of the liquid water content in the cloud. At longer wavelengths τ_λ depends also on the gaseous components of the cloudy layer. The parameters we need for equations (1.13) and (1.14) to find the SW fluxes, are: κ_λ^a and κ_λ^{abs}, where $\kappa_\lambda^{\prime} = \kappa_\lambda^{\prime}$ (gases) $+\kappa_\lambda^{\prime}$ (drops). The contribution due to the gases can be calculated for each wavelength interval as a function of the absorber amount. (See, for example, Rogers and Walshaw, 1966.) The contribution due to drops is calculated from the following expressions:

$$\rho\, \kappa_\lambda^{\prime} = \int_0^{\infty} N(a)\pi a^2 Q^{\prime}(\Delta\gamma) da \tag{1.16b}$$

$N(a)da(m^{-3})$ is the number of drops in the radius interval $(a, a+da)$ per unit volume. The "efficiencies"; i.e., the functions $Q^{abs}(\Delta\gamma)$ and $Q^{ext}(\Delta\gamma)$ are shown in Figures 1.6 and 1.7. Notice from these efficiencies (see equation (1.2)) that extinction by spheres becomes important for $\Delta\gamma \geq \approx 4$, and that, for constant index of refraction, $Q^{ext}(\quad \Delta\gamma)$ approaches 2 as the radius of the sphere increases. The absorption efficiency, Q^{abs} is shown for constant index of refraction. As we will see below, liquid water absorbs preferentially at certain wavelengths, so the absorptivity of a drop is not a simple function of a.

$$\omega_0^\lambda = \frac{\kappa_\lambda^{ext} - \kappa_\lambda^{abs}}{\kappa_\lambda^{ext}} \tag{1.16c}$$

$$\text{and } g_\lambda = \frac{\int_0^{\pi} \sin\theta d\theta \int_0^{\infty} N(a)\pi a^2 \cos\theta\, Q^{sc}(\Delta\gamma) da}{\int_0^{\infty} N(a)\pi a^2 Q^{sc}(\Delta\gamma) da} \tag{1.16d}$$

The radiative transfer equations allow us in principle to calculate all the effects of the passage of SW and LW radiation through horizontally uniform, infinite clouds in terms of these parameters.

Since it is difficult to calculate the parameters in equations (1.16) exactly, it is often useful to use approximations for them, and we discuss these in the next section.

II. Clouds and Radiation: Parameterization and Results

A. Solar Radiation Parameterizations

Useful approximations for ω_0^λ, g_λ, and τ_λ, which are needed to be able to solve equations (1.13) and (1.14), are often found by noting from Figure 1.6 that $Q^{ext}(\Delta\gamma) \to 2$ for $\Delta\gamma \gg 1$. Thus for all λ small compared with the mean droplet radii (and this holds through most of the solar spectrum) we have from equations (1.16b) that for SW radiation the drop contribution to the optical depth is

$$d\tau_\lambda = d\tau \approx (2\pi \int_0^{\infty} N(a)a^2 da) dz \tag{1.16'}$$

We now express τ in terms of the parameters usually measured in clouds; i.e., (a) the local liquid water content,

$$q_l \left(\frac{kg H_2O}{kg\ air}\right)$$

$$q_l = \frac{\rho_l}{\rho_{air}} \frac{4\pi}{3} \int_0^{\infty} N(a)a^3 da \tag{2.1}$$

and (b), the liquid water path,

$$W(z', z)\left(\frac{kg}{m^2}\right) = \rho_{air} \int_z^{z'} q_l(z'')dz'' \tag{2.2}$$

where ρ_l and ρ_{air} are the densities of liquid water and air, respectively. We can define an effective radius for a droplet size distribution,

$$r_{eff} = \frac{\int_0^{\infty} N(a)a^3 da}{\int_0^{\infty} N(a)a^2 da} \tag{2.3}$$

(Stephens, 1978). Then from equations (1.16a) and (2.3) we see that for SW radiation in clouds

$$\tau(z', z) \approx \frac{3}{2} \frac{W(z', z)}{(r_{eff})(\rho_l)} \tag{2.4}$$

A typical value of r_{eff} in low-lying stratiform clouds is $\approx 5\ \mu$, and a typical average value of q_l is $\approx 5 \times 10^{-4}$ when the clouds are several hundred meters thick. Thus the total SW optical path in such clouds is approximately

$$\tau \approx \frac{3}{2}\frac{(5 \times 10^{-4})(200)}{(5 \times 10^{-6})(1000)} \approx 30$$

The other parameters we need for the SW equations (1.13-1.14) are g_λ and ω_0^λ. It turns out that the results are fairly insensitive to g_λ, and for realistic drop size distributions $g \approx 0.85$ for all λ in the solar range. The specification of ω_0^λ is somewhat more important. ω_0^λ is defined by equation (1.16c) and includes scattering by drops, absorption by drops, and absorption by gases (mainly water vapor, ozone, and carbon dioxide). Most of the absorption of SW radiation is due to drops, so that to first approximation absorption due to gases can be neglected. $\omega_0^\lambda \approx 1$ always; however, the results of the calculations are very sensitive to ω_0^λ; due to multiple scattering, inside a cloud of $\omega_0^\lambda = .999$ (or an absorption probability event = .001) there can be considerable absorption of electromagnetic energy. For practical calculations of cloud reflectivity ω_0^λ is often put equal to 1, whereas for calculations of SW absorption by clouds it is convenient to use the linear approximation $1 - \omega_0^\lambda = 0.85\, C_\lambda\, a$ (Twomey and Bohren, 1980) where a is the average drop radius and C_λ is a constant that depends on wavelength. C_λ is approximately zero in the visible and takes on values $.1 - 20\ cm^{-1}$ in the near infrared (Slingo, 1989).

B. Terrestrial Radiation Parameterizations

According to equations (1.5-1.6), we need κ_λ^{abs} and the absorber densities to find the properties of LW fluxes in clouds. The important gaseous absorbers are water vapor (for $6\ \mu m < \lambda < 20\ \mu m$); CO_2 (for $\lambda \approx 15\ \mu m$) O_3 (for $\lambda \approx 9.6\ \mu m$), and water vapor (for λ in the window region $10 - 12\ \mu m$). Water drops absorb at roughly the same wavelengths as vapor. The LW fluxes in clouds can be approximated by noting that for a very thin layer of optical depth $d\tau_\lambda$ we have

$$F_\lambda^\downarrow(d\tau_\lambda) = F_\lambda^\downarrow(0)(1 - d\tau_\lambda) + \pi B_\lambda d\tau_\lambda$$

(see equation 1.6), and a similar equation holds for $F_\lambda^\uparrow(d\tau_\lambda)$. For a finite, homogeneous layer whose optical depth is not too great, we can approximate the fluxes in terms of two functions called emissivities, $\varepsilon_\lambda^\uparrow$ and $\varepsilon_\lambda^\downarrow$, such that the fluxes have similar behavior, namely

$$F^\downarrow(\tau_\lambda) = F^\downarrow(0)(1 - \varepsilon_\lambda^\downarrow) + \pi \bar{B}_\lambda \varepsilon_\lambda^\downarrow \tag{2.5}$$

$$F^\uparrow(\tau_\lambda) = F^\uparrow(\tau_\lambda^*)(1 - \varepsilon_\lambda^\uparrow) + \pi \bar{B}_\lambda \varepsilon_\lambda^\uparrow \tag{2.6}$$

where $\bar{B}_\lambda$ = the black body function at the mean temperature in the layer, and τ_λ^* = the total optical depth of the layer at wavelength λ. $\varepsilon_\lambda^\uparrow$ and $\varepsilon_\lambda^\downarrow$ are different because the spectral compositions of the upward and downward propagating beams are different. Fortunately, it turns out that to a fairly good approximation both $\varepsilon_\lambda^\uparrow$ and $\varepsilon_\lambda^\downarrow$ are independent of λ and of T, and that they take on the simple parameterised form

$$\varepsilon^\uparrow(z, z') \approx 1 - \exp[-a^\uparrow W(z, z')], \quad \varepsilon^\downarrow(z, z') \approx 1 - \exp[-a^\downarrow W(z, z')] \tag{2.7}$$

where $a^\uparrow \approx 158\ \frac{m^2}{kg}$, $a^\downarrow \approx 130\ \frac{m^2}{kg}$, and $W(z, z')$ is defined by equation (2.2). More detailed calculations are given by Roach and Slingo (1979).

Note that a truly black body, in these terms, has $\varepsilon^\uparrow = \varepsilon^\downarrow = 1$. Thus only for $W \geq 0.1\ \frac{kg}{m^2}$ is it a good approximation to assume clouds are black bodies (see Figure 2.4, below). Low-level stratiform clouds must be hundreds of meters thick for W to be this high.

C. Results for Warm, Plane-Parallel Clouds

Insertion of the parameterizations (equations 2.1-2.7) into the equations of radiative transfer (or, alternatively, using more accurate expressions for the necessary parameters) allows us to solve the equations for the SW and LW fluxes at any point within the cloud layer and on its boundaries. Of particular interest usually (as discussed in section I.b) are the following quantities: the SW reflectivity (or albedo), r, the SW transmittance, t, both integrated over all solar wavelengths; and the SW and LW cooling rates, where

$$r \equiv \frac{F_{sw}^\uparrow(0)}{\pi\mu_0 F_0^\downarrow(0)} \tag{2.8}$$

$$t \equiv \frac{F_{sw}^\downarrow(\tau^*)}{\pi\mu_0 F_0^\downarrow(0)} \tag{2.9}$$

the SW absorptivity, $a \approx 1 - r - t$, and the SW and LW cooling rate profiles are given by equation (1.7). Figures 2.1-2.4 show the results of such calculations. τ, and thus r, increases with cloud depth and with the total drop surface area, so that for given q_l a cloud made up of many small drops reflects more solar radiation than does one of a few large drops. r also increases with zenith angle θ_0. Figure 2.3 shows the spherical albedo (which is related to the reflectivity r) for clouds of varying τ and ω_0 and relates these to N, for a cloud of N drops/cm^3. According to this Figure, the overall trend is for increase of reflectivity with N for constant ω_0 and for increase of reflectivity with ω_0 at constant N.

The dependence of reflectivity on ω_o and N implies that changing either (via pollution, for example) may alter cloud reflectivity. The cloud absorptivity (for both LW and SW radiation) depends in part on pollutant levels; absorbing gases and carbonaceous particles within and between cloud drops can increase κ^{abs} and decrease ω_o considerably. Because of the difficulty in measuring absorptivity, it is not clear to what extent anthropogenic activity is altering the absorptivity of low-level clouds at present. The heating/cooling rates (equation 1.7) depend on absorption by drops (which depends on drop volume) and on absorption by gases, principally water vapor. SW absorption by liquid water and by water vapor are comparable. SW absorption in low-level stratiform clouds is usually maximum near the middle or in the lower half of the clouds, producing local warming there. Figure 2.4 shows both the SW reflectivity r (equation 2.8) and the LW effective emissivity ε (an average of $\varepsilon^\uparrow$ and $\varepsilon^\downarrow$ in equation 2.7) as functions of liquid water path W (equation 2.2) for $\theta_0 = \cos^{-1}(\mu_0) = 30°$. Typical low-level layer clouds have $\varepsilon \approx 0.9$, $r \approx 0.5$. LW absorption is strongest near cloud base and there is cooling near cloud top where the outgoing flux, $F^\uparrow(0)$, is not balanced by the downward flux. This imbalance is felt within the top 10-100 meters of these clouds. Further down inside the clouds, the fluxes become isotropic and the clouds radiate like black bodies. The SW heating and LW cooling rates are often comparable in magnitude ($\approx$ 6-10 K/hr) in low-level stratocumulus, but because they are concentrated at different heights within the clouds they give rise to convective motions important for cloud evolution.

D. Observations of Radiative Properties of Clouds

We now understand in a general way the theoretical relationships linking cloud properties to the impacts of clouds on LW and SW fluxes. This observation of cloud physical properties (cloud thickness, $q_l(z)$, $N(a, z)$, etc.) permits prediction of cloud albedos and heating rates, and observation of the radiative properties of clouds allows inference of the cloud microphysical parameters. By flying aircraft through clouds and simultaneously measuring the cloud radiative fluxes from satellites, for example, the theoretical relationships among the parameters can be tested and information on the current role of clouds in climate can be gleaned. We now discuss studies in which these relationships are used to interpret observations.

Satellite measurements consist of maps of upward directed fluxes in a range of wavelengths. Typically, fluxes are measured at 10–12 μ (the so-called "thermal" wavelengths), at 3–5μ (the near IR), and at the peak of the visible spectrum, near 0.6 μ. The spectrum of the radiation at around 10-12 μ is used to infer the temperature of the source (equation 1.1). Note that radiation in this wavelength region (called the "window" region) is absorbed very weakly in the clear sky (as shown in Figure 1.1). Thus the intensity of the upwelling thermal

radiation is a good measure of the temperature T of the source; i.e. cloudtop or Earth's surface. Subtraction of the black body radiation $B_\lambda(T)$ from the fluxes received at other wavelengths λ then leaves the intensity of short wavelength radiation reflected from the cloudtop or surface. At visible wavelengths near the peak of the SW radiation, ($\lambda \approx 0.5$–$0.6\ \mu$), droplet absorption is nearly zero (see Figure 4.4) and the cloud reflectivity r is determined by the cloud thickness and q_l (see equations 2.1-2.4). The reflectivity at visible wavelengths is nearly proportional to W (equations 2.1-2.4). At longer wavelengths, ($\lambda \approx 1$–$5\ \mu m$) absorption by droplets in the upper part of the cloud lowers the SW flux reaching, and thus being backscattered by, cloud droplets in the cloud interior, so the reflectivity at these wavelengths is due only to droplets in the upper part of the cloud. It therefore does not depend on cloud thickness for clouds more than 50 m thick, and decreases (as absorption increases: see Figure 1.7) with mean cloud droplet size. Thus by looking at fluxes in different wavelength intervals we obtain different kinds of information.

Figure 2.6 shows the relationships between observed values of cloud liquid water path (as measured by the quantity $\frac{W}{\mu_o \rho_l}$) and cloud reflectivity, at 0.63 μ from the NOAA Advanced Very High Resolution Radiometer (AVHRR) for clouds off the coast of California. The cloud albedo is ≈ 0.4–0.5 for a range of values of W. This range is typical for marine stratocumulus. Figures 2.7 and 2.8 show the cloud reflectivity at 0.63 and 3.7 μ (corrected for thermal radiation) as functions of total aerosol count (observed from aircraft). The high peaks in N in Figure 2.7 are due to shipstacks and in Figure 2.8 to urban air. The figures are thus evidence that one result of increasing pollution may be to increase the SW albedo of low-level stratiform clouds.

Figure 2.9 shows observed and calculated LW heating/cooling rates (equation 1.7) for a nocturnal stratocumulus case. The cooling is very strong in the upper 100 m or so of the cloud, because there is virtually no downward LW or SW flux at cloudtop. Heating is strongest at cloudbase, due to absorption of terrestrial radiation there.

We have assumed in our theoretical treatment that we are always dealing with unbroken, horizontally uniform cloud How then can these theories be used to interpret observations that are often of broken, inhomogenous layers? This is a much larger subject than we shall go into here, but we show two observational methods for the identification of broken cloud fields. First, since both unbroken clouds and open ocean are quite uniform, we can use the standard deviation of the thermal radiation to give a measure of the standard deviation of the temperature (and thus the altitude) of the radiating surface. Figure 2.10a shows a plot of the local standard deviation σ of each "measurement," where each "measurement" is the average 11 μ radiance in a 4×4 (1 km^2) array of AVHRR data. The two low σ regions correspond to clear sky and unbroken clouds, respectively, and the high σ region in the middle corresponds to broken clouds. Another means for identification of different sorts of cloud regions is to graph local mean reflectivity in the visible against the IR radiance, as shown in Figure 2.10b. Cloud-free regions are characterized by low reflectivity in the SW but emit thermal radiation characteristic of the ocean surface. Unbroken clouds emit less thermal radiation, since they are cooler than the sea surface, but they are highly reflective. Pixels corresponding to intermediate values of both reflectivity and thermal radiance are representative of broken clouds. It is clear from both figures that broken cloud fields are very different, radiatively, from unbroken fields, and they must be accurately parameterized in climate models.

III. The Climatic Impacts of Clouds

There are three kinds of questions we can now address with the tools we have developed, namely: What, if any, is the role of clouds in modifying the net radiation balance of the Earth-atmosphere system? What, if any, is the role of clouds in modifying the distribution of heating and cooling within the atmosphere and at the Earth's surface? What, if any, are the impacts of radiative fluxes on cloud properties? We consider the first two very briefly here and the third in the next chapter.

A. The Impact of Clouds on Global Radiative Balance

A simple energy budget of the Earth-atmosphere system can be stated as follows:

$$R_{net} = S_0(1 - a_s) - OLR \tag{3.1}$$

R_{net} is the net rate of energy (Watts/m^2) incoming or outgoing at the top of the atmosphere, S_0 is the energy flux in the solar beam, OLR is the outgoing LW radiation flux there, and a_s is the system albedo. We have seen that clouds modify both a_s and OLR, increasing a_s and decreasing OLR over the clear sky value. An increase in a_s clearly decreases R_{net}, causing a net cooling of the system, whereas the decrease in OLR heats the system. We can rewrite equation (3.1) as follows:

$$R_{net}(with\ clouds) = S_0[1 - a_s(with\ clouds)] - OLR(with\ clouds)$$

$$R_{net}(without\ clouds) = S_0[1 - a_s(no\ clouds)] - OLR(no\ clouds)$$

The effect of clouds on global radiation balances is then

$$R_{net}(with\ clouds) - R_{net}(without\ clouds) \equiv \Delta R_{net_{due\ to\ clouds}} = -S_0[a_s(with) - a_s(without)] - [OLR(with) - OLR(without)]$$

It is important therefore to ask which effect dominates in the current atmosphere and which is likely to dominate in the foreseeable future.

From equation (2.6) we see that for low-lying thick clouds $F^\uparrow(0)$ is not too different from $\pi B_\lambda(\bar{T})$, and for low-lying thin clouds $F^\uparrow(0) \approx F^\uparrow(\tau_\lambda^*) = \pi B_\lambda(T_G)$. Thus for both thin and thick low-lying clouds (since $\bar{T} \approx T_G$) the OLR is not very different from the OLR for clear skies. On the other hand, we have seen (Figures 2.2-2.4) that a_s (clouds) $> a_s$ (clear sky). Thus for low-level clouds the SW effect dominates: these cause $R_{net} < 0$ and represent a cooling influence.

Clouds in the upper atmosphere also have $a_s > a_s$ (clear sky). However in this case $\bar{T} < T_G$ (since the in-cloud temperature $\bar{T}$ at any altitude $\approx$ the temperature of the clear air at that altitude), so OLR (clouds) < OLR (clear sky). Therefore upper level clouds may either heat or cool the system.

A satellite study (Ramanathan et al., 1989) of R_{net} shows that, averaged over all clouds and over the whole Earth, $\Delta R_{net_{due\ to\ clouds}} < 0$: at present, clouds cool the Earth-atmosphere system. This is the result of the low-level clouds, and hence it is important to ask whether low-level cloud cover is apt to increase or decrease in the future as the Greenhouse Effect increases. It has been suggested (Charlson et al., 1989) that one effect of rising temperatures (due to injection of greenhouse gases into the atmosphere, for example) may be to increase the biological production rate of CCN and thus to increase low cloud cover. Either the increase in albedo of existing clouds, or the increase in low cloud cover, or both, would produce negative feedbacks in the climate system, decreasing the amount of SW flux reaching the surface and thus counteracting, in some measure, the warming trend.

B. The Impact of Clouds on Surface Temperature

Surface warming due to clouds is due to emission of LW radiation downward from cloud base. We can very roughly estimate the magnitude of this effect for different kinds of clouds by considering a cloud layer which has SW reflectivity r, LW emissivity $\varepsilon \approx 1$, and temperature T_1. First let us imagine this is a low cloud, as pictured in Figure 3.1a. If $F^\downarrow_{LW}(0) = 0$, we have from equation (2.6) that, integrating over the LW spectrum,

$$F^\uparrow_{LW}(0) = \sigma T_1^4 \approx \sigma T_g^4 \tag{3.2}$$

The condition of energy balance for the system is

$$\frac{(1 - r)S_0}{4} = \sigma\ T_1^4 \approx \sigma T_g^4 \tag{3.3}$$

Thus we find that

$$T_G^{(low\ cloud)} = \left[\frac{(1-r)S_0}{4\sigma}\right]^{\frac{1}{4}} \tag{3.4}$$

If the cloud had been absent, we would have found

$$\sigma T_G^4 = \frac{S_0(1-r_0)}{4}, \quad T_G\ (no\ cloud) = \left[\frac{(1-r_0)S_0}{4\sigma}\right]^{\frac{1}{4}}$$

so the surface cooling in this case is

$$\Delta T_G\ (low\ cloud) = \left(\frac{S_0}{4\sigma}\right)^{\frac{1}{4}}\left[(1-r)^{\frac{1}{4}} - (1-r_0)^{\frac{1}{4}}\right] \tag{3.5}$$

Average values of r for low clouds ≈ 0.5, whereas over the sea $r_0 \approx 0.1$–0.15. Thus ΔT_G (low cloud) ≈ -20 K over the sea.

Now suppose the same cloud lies in the upper troposphere, so that its temperature $T_1 \neq T_G$ (see Figure 3.1b). Let us assume the subcloud layer, like the cloud, absorbs all the LW radiation and none of the SW radiation incident upon it. We find by very similar reasoning, assuming the subcloud layer is a black body at constant temperature, that

$$\Delta T_G\ (high\ cloud) = \left(\frac{S_0}{4\sigma}\right)^{\frac{1}{4}}\left[[2(1-r)]^{\frac{1}{4}} - (1-r_0)^{\frac{1}{4}}\right] \tag{3.6}$$

Using the same values of the parameters we find that the surface heating due to the high cloud is positive, while that due to the low cloud is negative. This is due to the radiative effects of the subcloud layer; since the water vapor is concentrated in the lowest atmospheric layers, a low cloud does not add significantly to the Greenhouse effect. However, adding a cloud to upper, drier layers, can substantially increase this effect. Figures 3.2 and 3.3 show some more careful calculations of the impacts of clouds on surface temperatures.

IV. Effects of Radiative Fluxes on Clouds

We have now seen that the interactions of clouds with radiative fluxes modifies the temperatures of the surface and atmosphere below and in the clouds. These modifications are not static because in the process the radiative fluxes change the cloud properties as well. We now investigate these changes.

A. Macrophysical Effects

The absorption and emission of energy inside clouds changes the local temperature, which changes the buoyancy of cloud air. In some circumstances this substantially modifies cloud dynamics.

Consider a layer of cloud of thickness h, at temperature T_c, which radiates through its upper surface into a medium of temperature $T_A = T_c - \Delta$. The rate of change of the layer temperature is roughly

$$\rho c_p \frac{dT_c}{dt} \sim \rho c_p \frac{d\Delta}{dt} = \sigma \frac{(T_A^4 - T_c^4)}{h} \approx -4\sigma T_c^3 \frac{\Delta}{h}$$

Thus

$$\frac{d\Delta}{dt} = -\frac{\Delta}{t_{rad}} \tag{4.1}$$

where

$$t_{rad} = \left[\frac{4\sigma T_c^3}{\rho c_p h}\right]^{-1}$$

$T_c \approx 270$ K, $h \approx 100$ m. Thus the time for the cloud temperature to change a few degrees via radiative loss to the upper atmosphere is approximately

$$\frac{t_{rad}}{270} \cdot 2 \approx \frac{10^5}{4(5\times 10^{-8})(20\times 10^6)} \approx \frac{2}{270}$$

or a few minutes, in the absence of other effects. This is the length of time it would take to [illegible]y the temperature and thus the dynamics of the cloud substantially by radiative cooling alone. It is long compared with time scales for motion of convective cloud parcels out of the radiatively active regions. Thus for most convective clouds radiation does not have important impacts on cloud dynamics. However, for very large layer clouds, which last for days and in which circulations are very slow, radiation becomes an important heat source/sink which modifies the temperature profile in the cloud and thus the cloud motions. In marine stratocumulus, for example, circulation of air carrying heat and moisture from the sea is driven in part by radiative cooling of cloudy air near cloudtop. This becomes the major source of turbulent kinetic energy in nocturnal clouds. When for any reason the net cooling is diminished, either by the presence of clouds aloft (which contribute downward IR fluxes at cloudtop) or by heating due to absorption of solar radiation, then the circulation weakens. Figures 4.1 and 4.2 show the diurnal variation of cloud amount and cloudtop temperature from GOES E and W (Minnis and Harrison (1984)), showing a distinct diurnal cycle with cloud thinning in the afternoon. This is not due to "burnoff" or evaporation of the drops in place, but is probably due rather to the dynamic effect of absorption of solar radiation in the lower half of the cloud, coupled with the radiative cooling near cloudtop. This situation leads to a slight inversion forming near cloudbase that cuts off the flux of moisture from below, while convection is maintained in the cloud by the heating-cooling "dipole." Turton and Nicholls (1987) modelled this cloud thinning via solar heating and produced the realistic looking curves shown in Figure 4.3. The possibility of this decoupling of the cloud from the surface must be considered in any model of clouds and radiation.

B. Microphysical Effects

Both water drops and water vapor absorb radiation. It is partially re-emitted, partially used to evaporate the drops, and partially given off via conduction to the moist air between the drops. Davies et al. (1984) showed that typical boundary layer clouds absorb about 9% of the extraterrestrial insolation and that 75-90% of this absorption is due to the droplets, rather than the vapor. Figure 4.4 shows calculated values of ω_o^λ for a layer cloud consisting only of drops and for one consisting of drops + vapor. Evaporation of water into the moist air and conduction heating of the air change the supersaturation, as shown in Figure 4.5, which then further modifies the rate of nucleation, evaporation, or condensation. Thus the effects of radiative fluxes on cloud droplets are complex. They modify droplet numbers and sizes, thus modifying the fluxes themselves (since absorption and scattering of radiation by drops are highly size dependent: see Figure 1.6).

Thus to assess climatic effects of the cloud-radiation interactions we must take into account modification of the clouds by the radiative fields as well as a modification of the radiative fields by the clouds. In other words, calculations of the effects of, say, CO_2 doubling, must include the feedbacks due to changes in the clouds caused by the perturbation in atmospheric radiative fluxes.

V. Summary

In these lectures we have reviewed the basic equations of radiative transfer in one dimension through horizontally-uniform clouds. These are first order linear differential equations with constant coefficients. The coefficients are functions of the material responsible for absorption and scattering of the radiation. They depend, in general, on wavelength, on gaseous composition, and on the number and size distribution of cloud droplets. Because they are difficult to calculate, we have presented some simple parameterisations which depend only on easily measured features of cloud layers.

We have briefly summarised the theoretical predictions for the SW reflectivity and for radiational heating rates in boundary layer clouds and reviewed some recent observations of these quantities. This discussion lead to consideration of the role of clouds in radiative climate, which we considered in terms of the impacts of clouds on heating of the Earth's surface and of the atmosphere. Our discussion here assumed that these effects could be considered in terms of static cloud properties, but in the last section we discussed changes in cloud macrophysical and microphysical properties that follow from the cloud-radiation interactions, and we showed that it is important to keep these cloud responses in mind in interpreting predictions of climate change.

References

Coakley, J. and F. Bretherton (1982) *J. Geophys. Res., 87*, 4917-4932.

Coakley, J. and J. Snider (1989) Proceedings, AMS Symposium on the Role of Clouds in Atmospheric Chemistry and Global Climate, Anaheim, pp. 175-177.

Davies, R. et al. (1984) *J. Atmos. Sci., 41*, 2126-2137.

Houghton, D. (1977) *The Physics of Atmospheres*, Cambridge University Press, 202 pp., p. 9.

Joseph, J. H., W. J. Wiscombe and J. A. Weinman (1976) *J. Atmos. Sci., 33*, 2452-2459.

Meador, W. and W. Weaver (1980) *J. Atmos. Sci., 37*, 630-643.

Minnis, P. and E. Harrison (1984) *J. Chem. Appl. Meteor., 23*, 1012-1031.

Minnis, P. et al. (1989) First ISCCP Regional Experiment Workshop, Monterey.

Ramanathan, V. et al. (1989) *Science, 243*, 57-63.

Roach, W. and T. Slingo (1979) *Quart. J. Roy. Meteor. Soc., 105*, 603-614.

Rodgers, C. and C. Walshaw (1966). *Quart. J. Roy. Meteor. Soc., 92, 67-92.*

Slingo, A. (1989). *J. Atmos. Sci. 46*, 1419-1427.

Slingo, A. and H. M. Schrecker, *Quart. J. Roy. Meteor. Soc., 108*, 407-426.

Stephens, G. (1978) *J. Atmos. Sci., 35*, 2123-2132.

Stephens, G. and P. Webster (1981) *J. Atmos. Sci., 38*, 235-47.

Turton, J. and S. Nicholls (1987) *Quart. J. Roy. Meteor. Soc., 113*, 969-1010.

Twomey, S. and C. Bohren (1980) *J. Atmos. Sci., 37*, 2086-2094.

Twomey, S. (1977) *J. Atmos. Sci., 34*, 1149-1152.

van de Hulst, H. C. (1957) *Light Scattering by Small Particles*, 471 pp., pp. 177 and 181.

Radke, L., J. Coakley, Jr. and M. King (1989) To be published, *Science*.

Durkee, P. (1989) Proceedings, AMS Symposium on the Role of Clouds in Atmospheric Chemistry and Global Climate, Anaheim, p. 157.

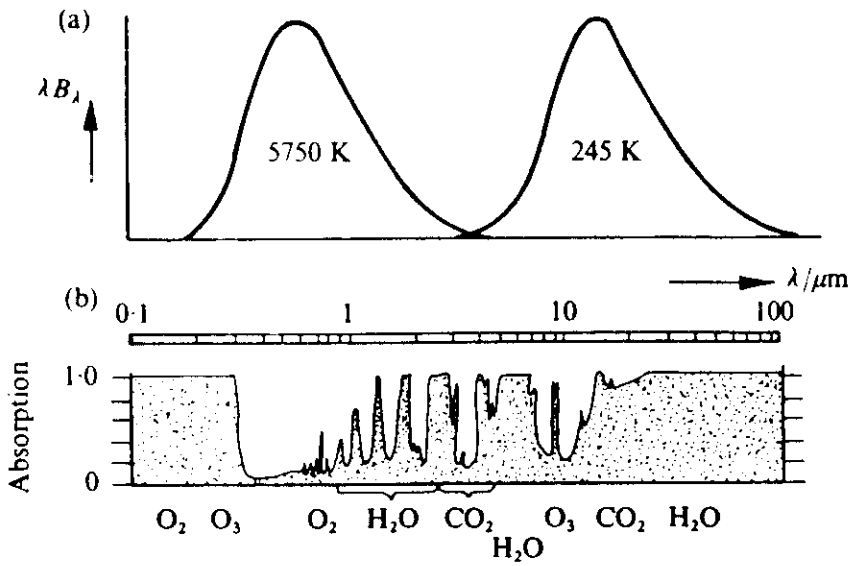

Fig. 1.1 (a) Curves of black-body energy B_λ at wavelength λ for 5750 K (approximating to the sun's temperature) and 245 K (approximating to the atmosphere's mean temperature). The curves have been drawn of equal areas since integrated over the earth's surface and all angles the solar and terrestrial fluxes are equal.
(b) Absorption by atmospheric gases for a clear vertical column of atmosphere. The positions of the absorption bands of the main constituents are marked. (From Houghton, 1977.)

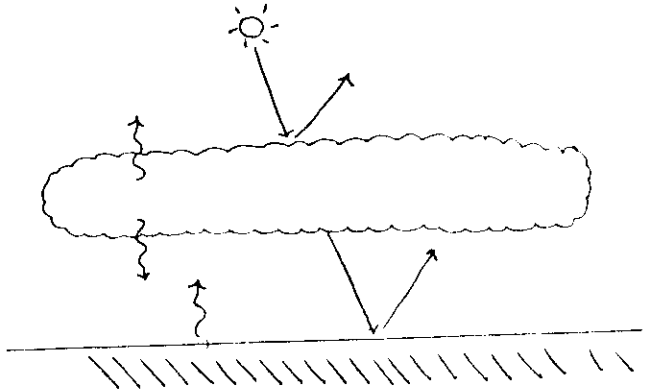

Fig. 1.2. The interactions of solar ($\longrightarrow$) and terrestrial ($\rightsquigarrow$) radiation with a horizontal cloud layer.

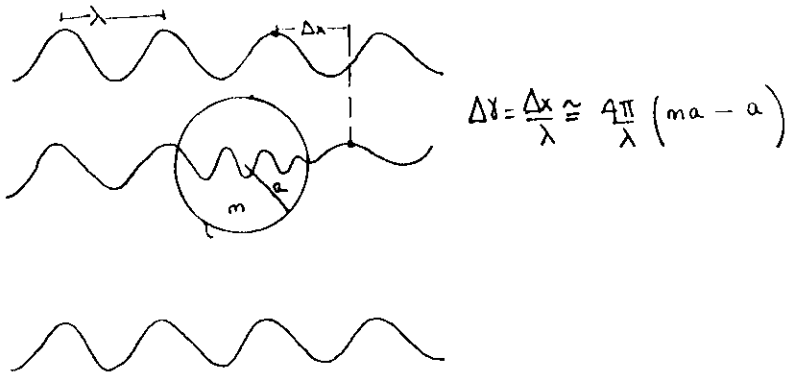

Fig. 1.3. The passage of photons of wavelength λ through a drop of radius a, index of refraction m. The difference in phase between the photons passing through the drop and those passing through clear air is $\Delta\gamma = 4\frac{\pi}{\lambda} a\,(m - 1)$.

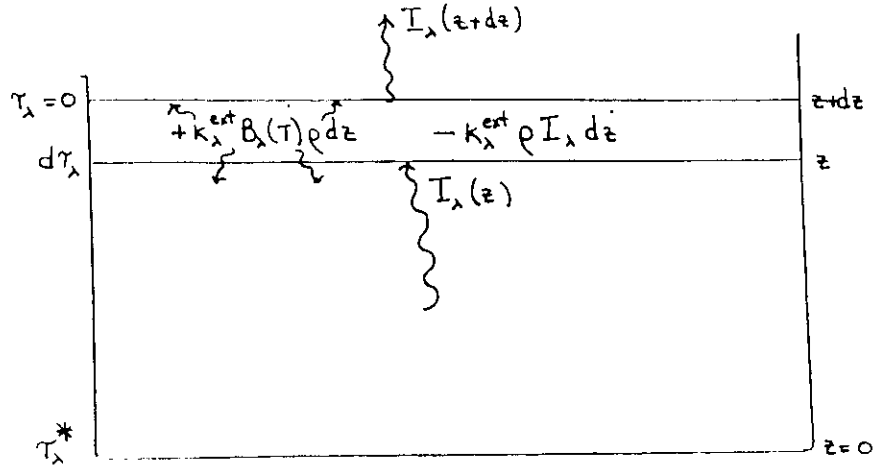

Fig. 1.4a. The absorption and reemission of monochromatic LW radiation by an infinitesimal uniform slab of material.

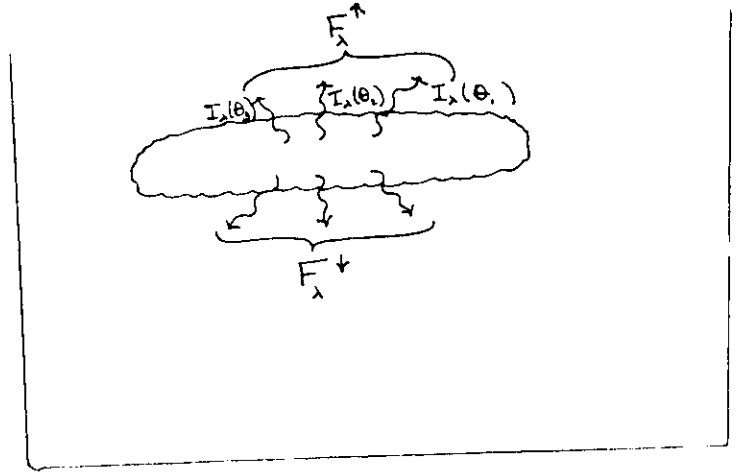

Fig. 1.4b. The definition of the fluxes $F_\lambda^\uparrow$ and $F_\lambda^\downarrow$.

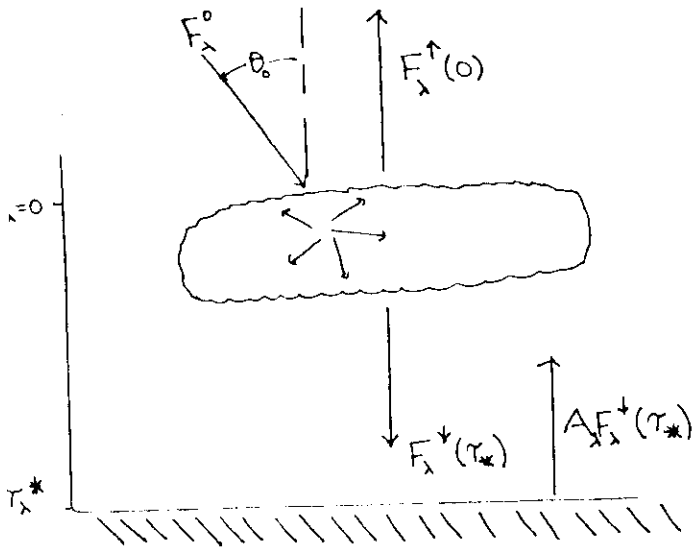

Fig. 1.5. Passage of solar radiation through a cloud. The upward and downward fluxes are integrated over the scattered intensities (see eq. 1.4). A_λ is the surface albedo and $\theta_0 = \cos^{-1}(\mu_0)$ the solar zenith angle.

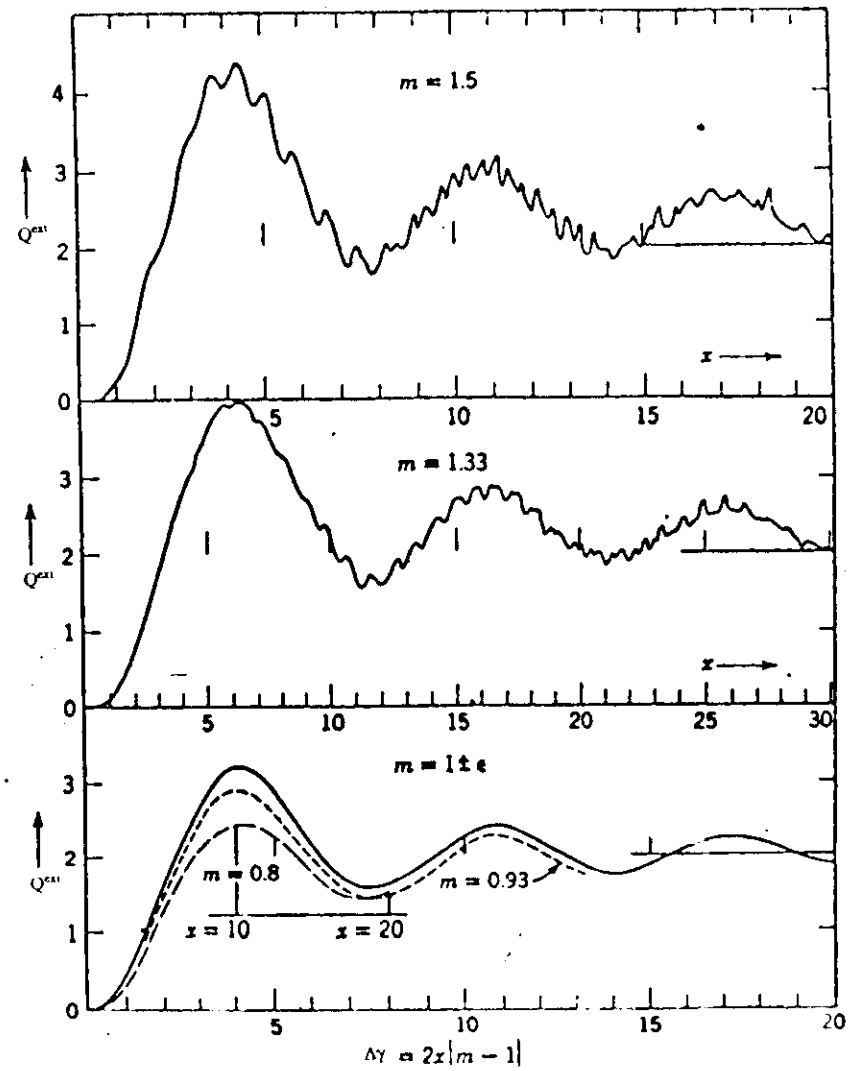

Fig. 1.6. Extinction curves computed from Mie's formulae for $m = 1.5$, 1.33, 0.93, and 0.8. The scales of $x = \frac{2\pi a}{\lambda}$ have been chosen in such a manner that the scale of $\Delta\gamma = \frac{4\pi a}{\lambda}(m-1)$ is common to these four curves and to the extinction curve for $m = 1 \pm \varepsilon$. (From van de Hulst, 1957.)

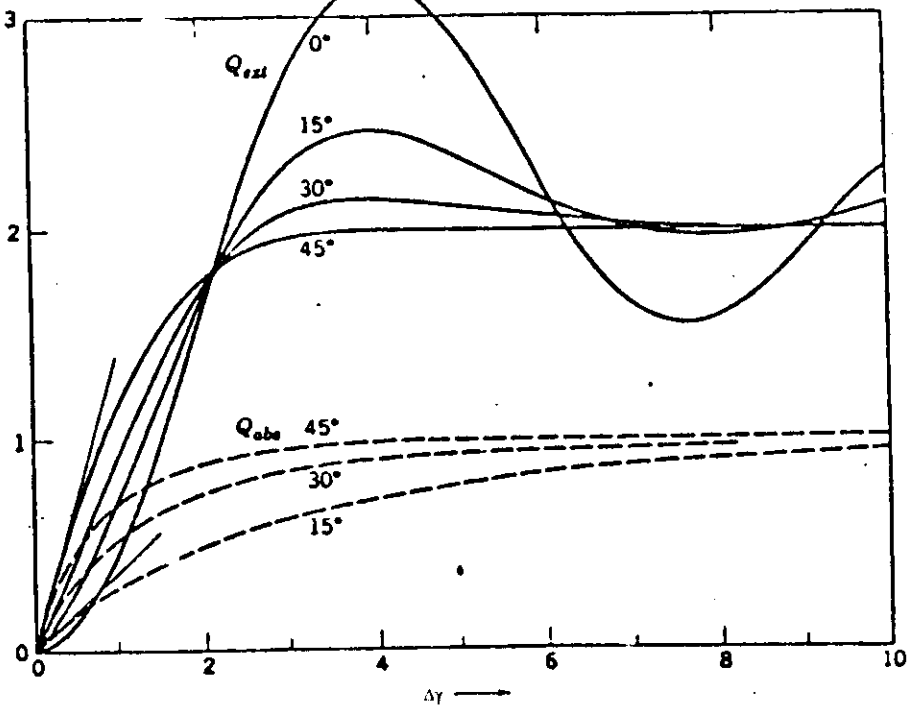

Fig. 1.7. Influence of an imaginary term in the refractive index upon the extinction curve for n close to 1. The refractive index is $1 + \varepsilon \cdot i\varepsilon \tan \beta$ (ε small). (From van de Hulst, 1957.)

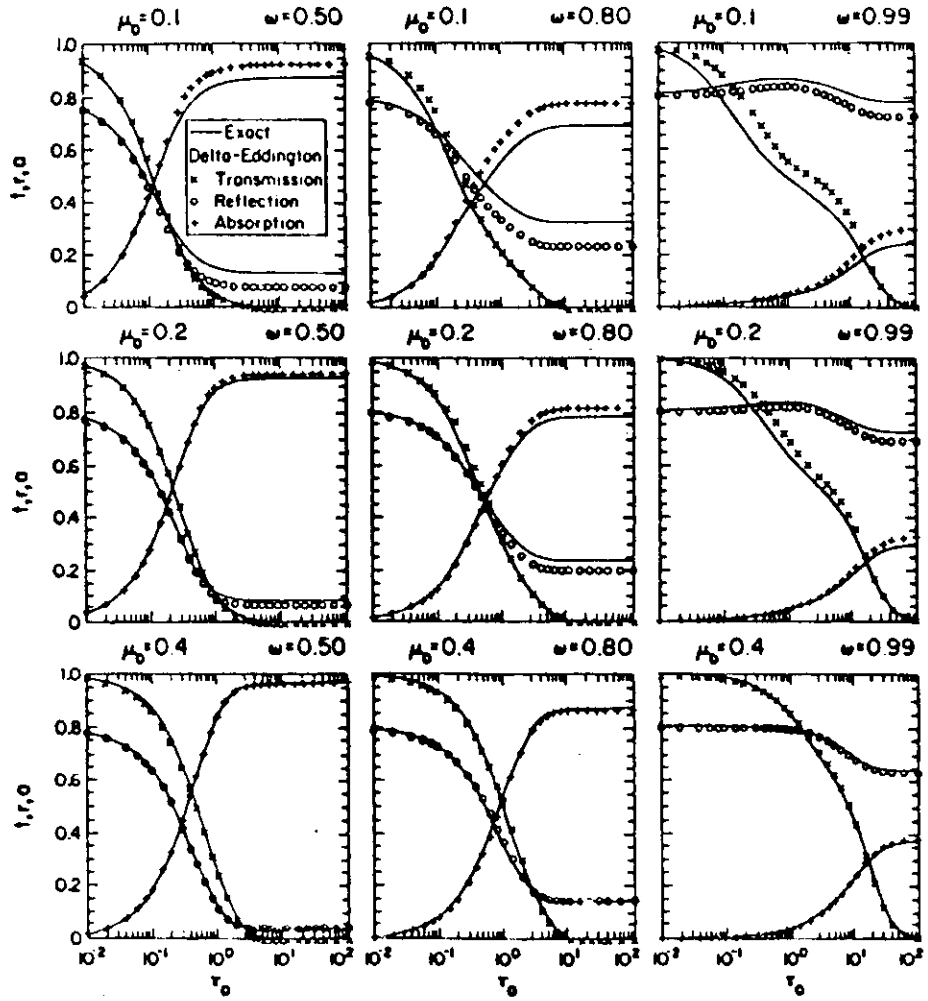

Fig. 2.1. Reflectivity (r), transmissivity (t) and absorptivity (a) versus layer optical depth τ_0 for a range of large solar zenith angles (μ_0) and single-scattering albedos (ω), comparing exact and delta-Eddington methods for asymmetry factor g = 0.85 and surface albedo A = 0.8. (From Joseph et al., 1976.)

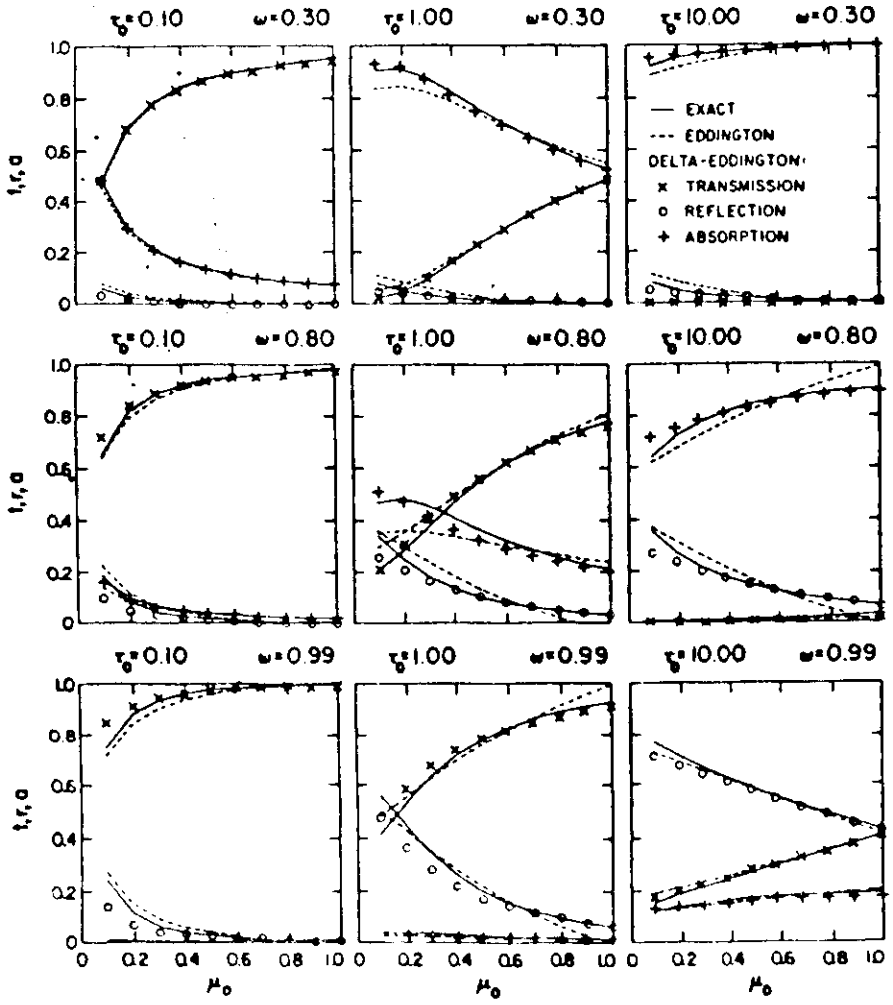

Fig. 2.2. Reflectivity (r), transmissivity (t) and absorptivity (a) as a function of sun angle μ_0 for various single-scattering albedos (ω) and layer optical depths (τ_0), comparing exact, Eddington and delta-Eddington methods for asymmetry factor g = 0.8 and surface albedo A = 0. (From Joseph et al., 1976.)

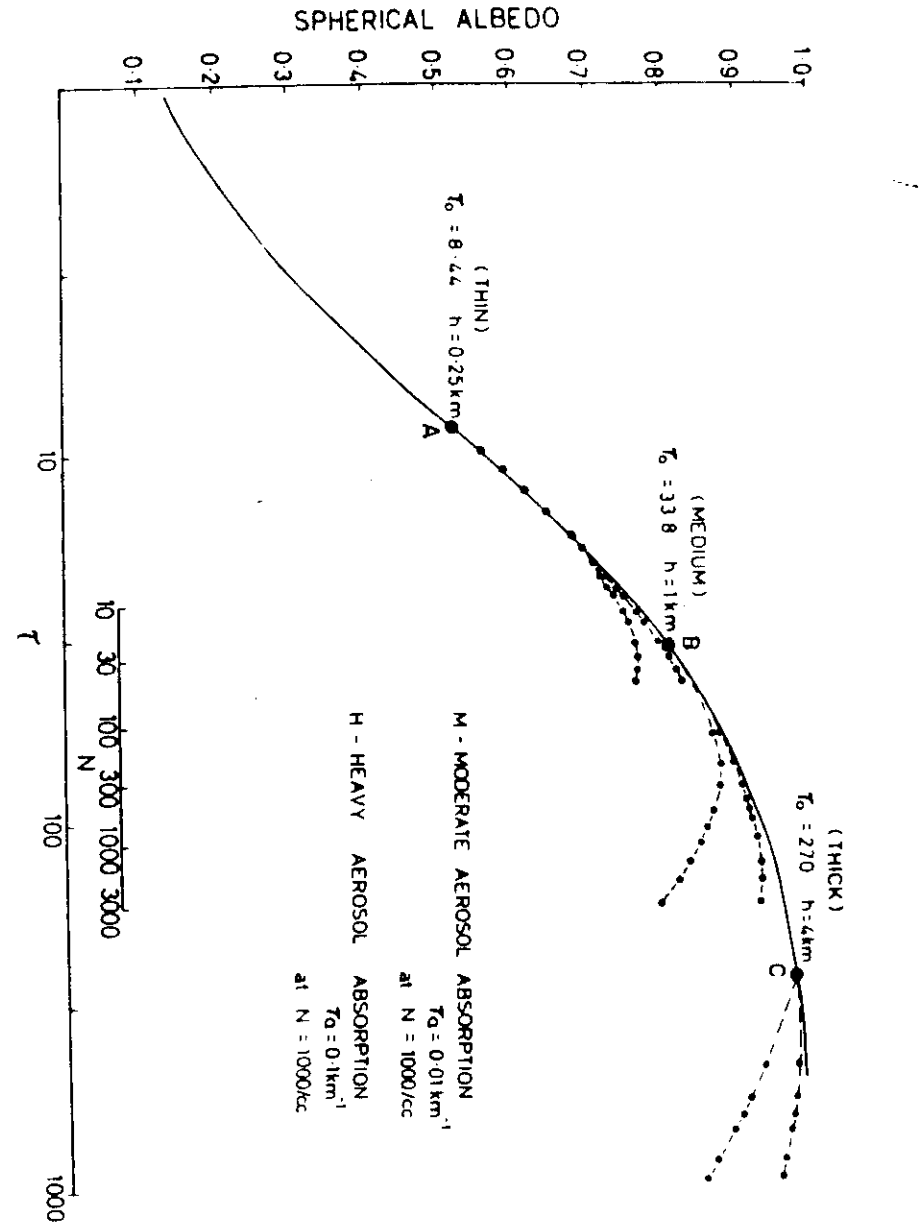

Fig. 2.3. Numerically computed trajectories corresponding to the schematic curves in Fig. 2. for the change of spherical albedo with increasing pollution for thin, moderate and thick clouds. (From Twomey, 1977.)

Fig. 2.4. Albedo and emissivity relationships as a function of the liquid water path (gm^{-2}). Curves represent the basics cloud optical property parameterization of Stephens (1978). The effective emittance is invariant with latitude. However, the cloud albedo is distinctly zenith angle dependent. Clouds which fall into the particular liquid water path range are shown on the upper abscissa. (From Stephens and Webster, 1981.)

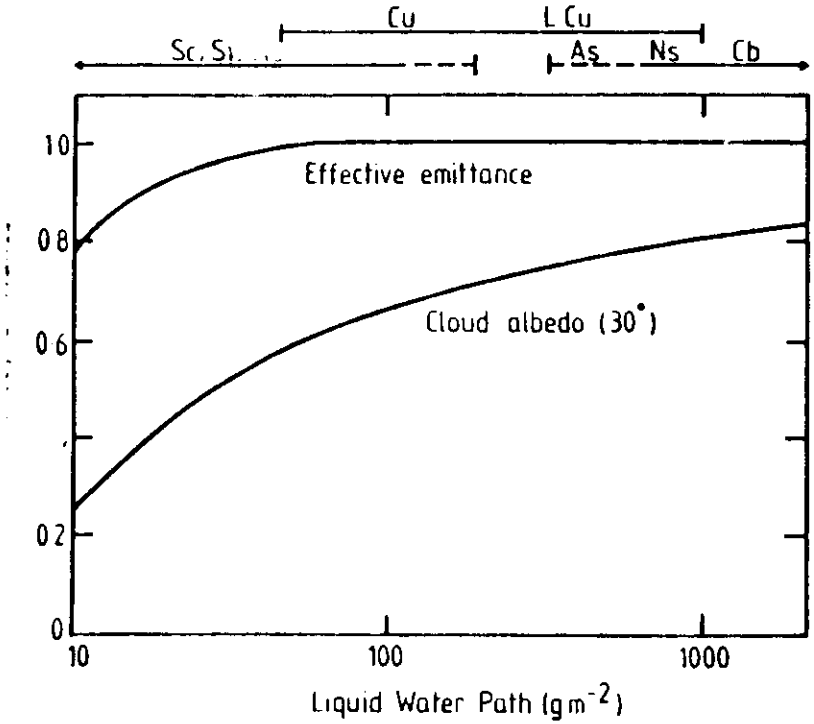

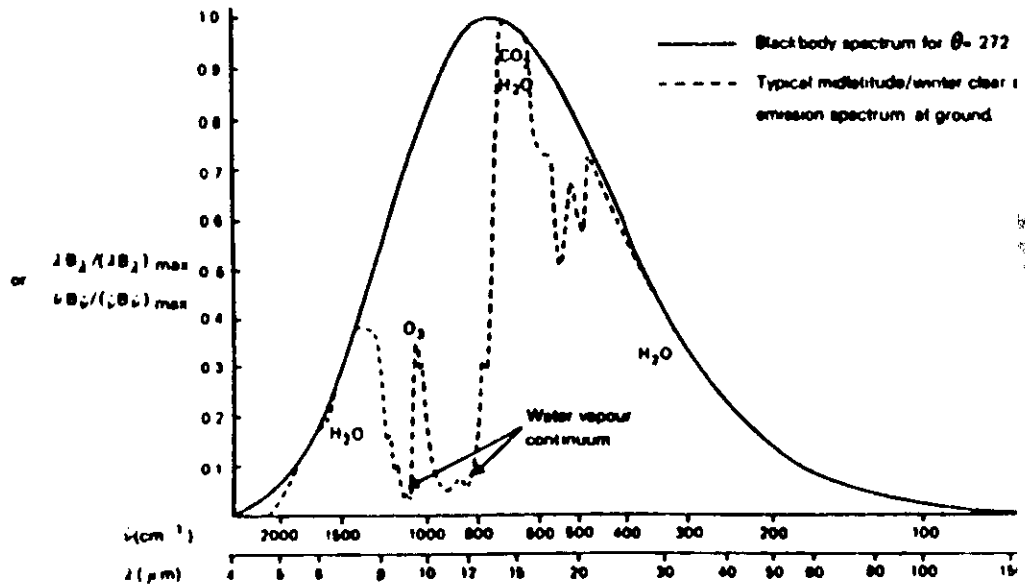

Fig. 2.5 Principal atmospheric absorbers of terrestrial radiation. Water droplets absorb throughout this wavelength region. (From Roach and Slingo, 1979.)

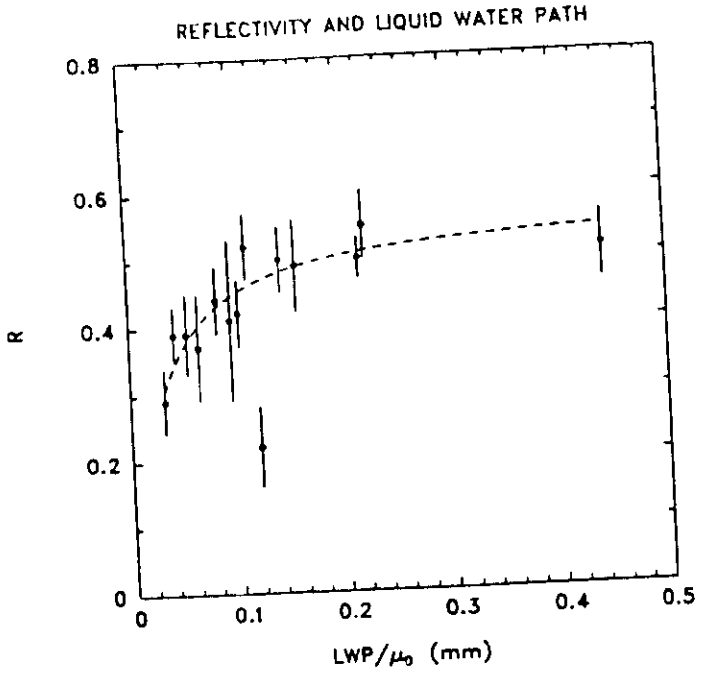

Fig. 2.6. Reflectivities and cloud liquid water paths. The error bars on the reflectivities indicate the standard deviation of the reflectivities for overcast fields of view. (From Coakley and Snider, 1989.)

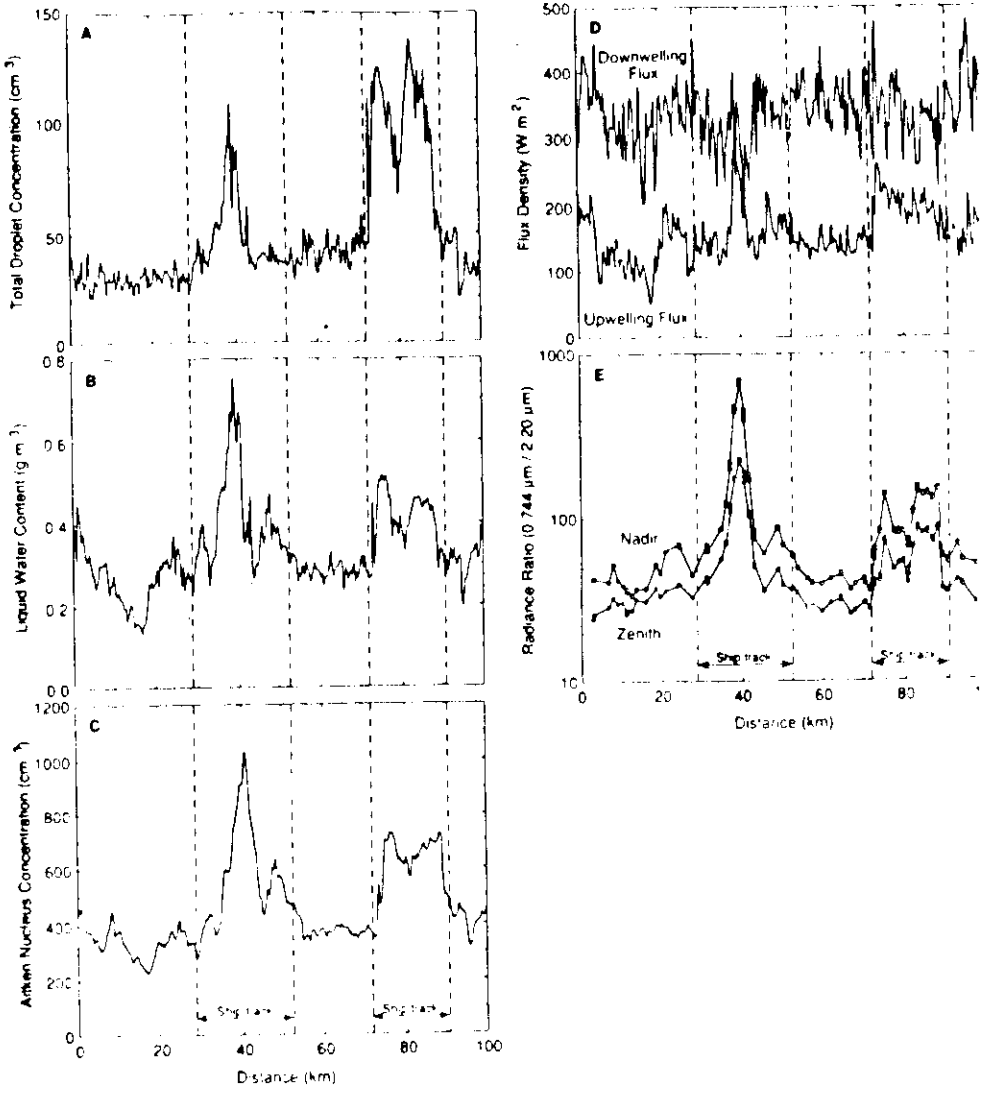

Fig. 2.7. (From L. Radke, J. Coakley, Jr. and M. King, *Science*, 1989.)

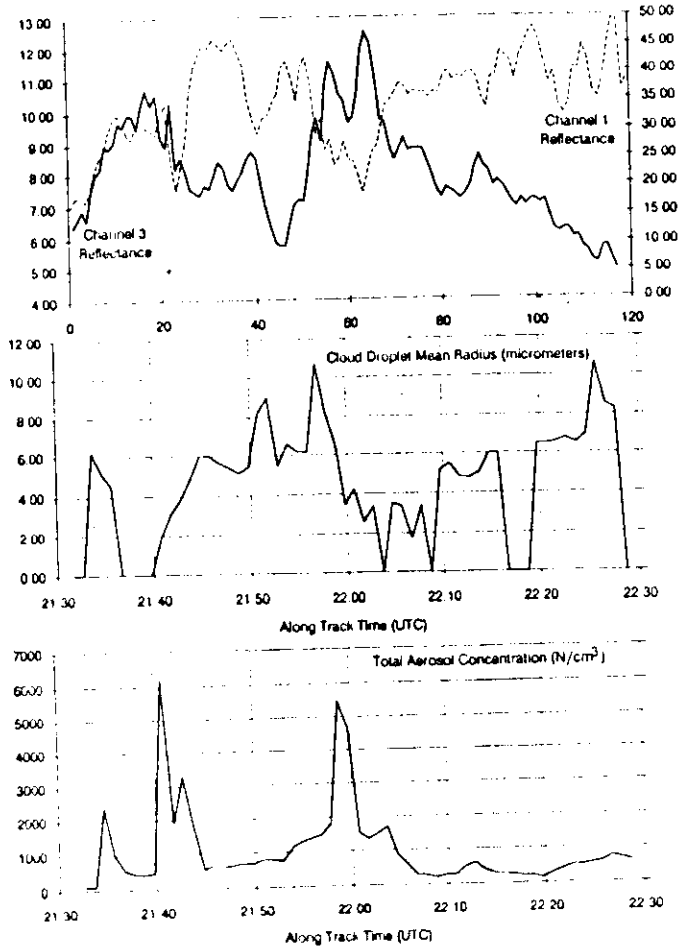

Fig. 2.8. Comparison of AVHRR channel 1 (0.63 μm) and 3 (3.7 μm) reflectance with aircraft-measured cloud droplet mean radius and total aerosol concentration. The satellite data are from NOAA 9 at 22:06 UTC on 10 July 1987. (From Durkee, 1989.)

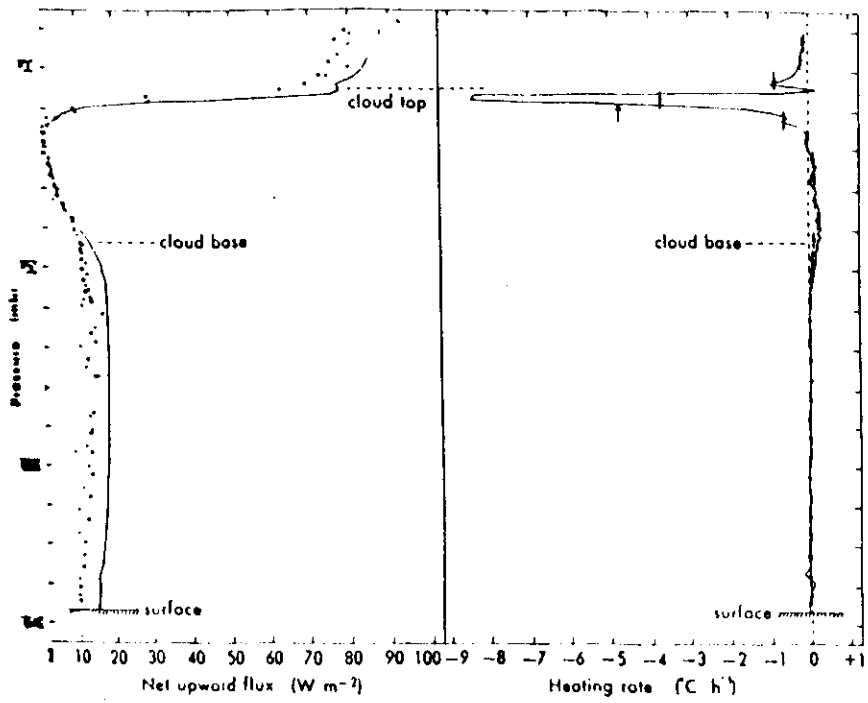

Fig. 2.9. Comparison of the observed and theoretical net infrared fluxes and heating rates for profile 1, November 1976. The continuous lines are from the radiation scheme, using the balloon temperatures, humidities and the scaled ASSP data. The dots and crosses represent the corrected fluxes from the upper and lower radiometers, respectively. Only every fifth value has been plotted. (From Roach et al.)

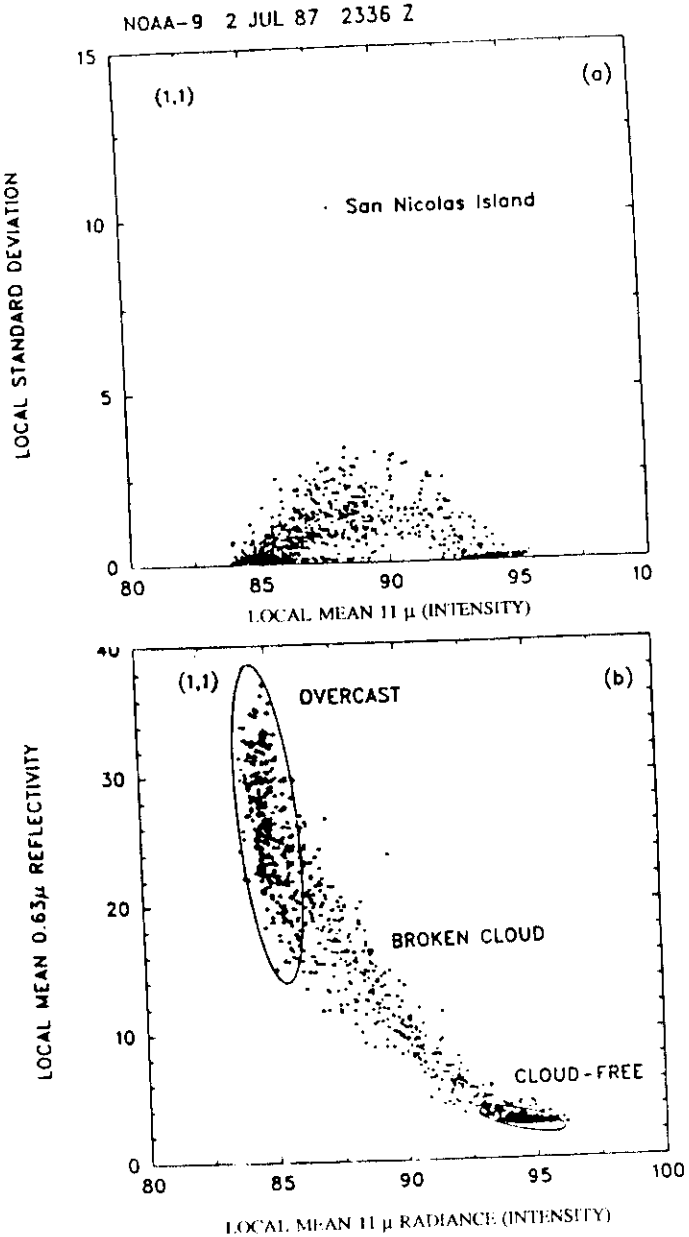

Fig. 2.10. Spatial coherence analysis of 11 μm radiances for $(250\ km)^2$ region containing San Nicolas Island (a) and corresponding 0.63 μm reflectivities (b). Each point is a $(4\ km)^2$ portion of the $(250\ km)^2$ region constructed by taking 4×4 arrays of $(1\ km)^2$ AVHRR data. The observations are for the NOAA-9 overpass on July 2, 1987. The ellipses in (b) surround points identified as being cloud free and completely cloud-covered.

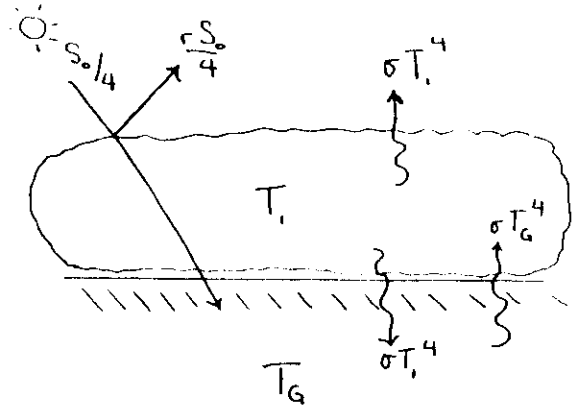

Fig. 3.1a. Energy balance for a low cloud which is transparent to solar radiation (⟶) but absorbs and reemits all the terrestrial radiation (⇝). Earth's albedo is 0 in this example.

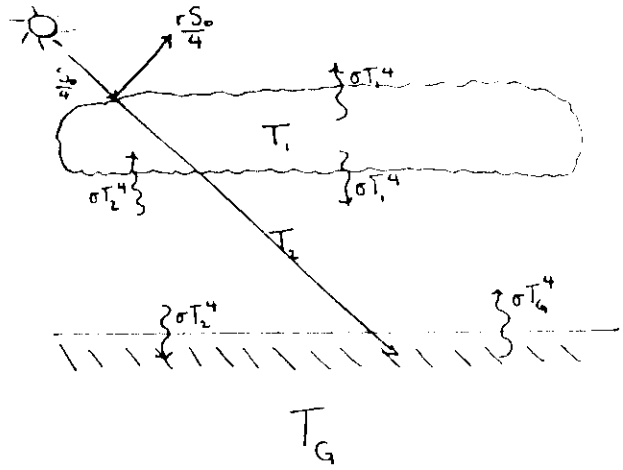

Fig. 3.1b. Energy balance for a high cloud above a clear subcloud layer. Both cloud and subcloud layers are transparent to solar radiation but both layers absorb and reemit all LW radiation incident upon them.

Fig. 3.2. Surface temperature difference between clear and overcast skies as a function of surface albedo. Results are for 5, 35, and 65°N in winter. Clouds possess the indicated liquid water path. The low (L), medium (M), and high (H) clouds occupy the same layers 913-854, 632-549, and 381-301 mb, respectively. (From Stephens and Webster, 1981.)

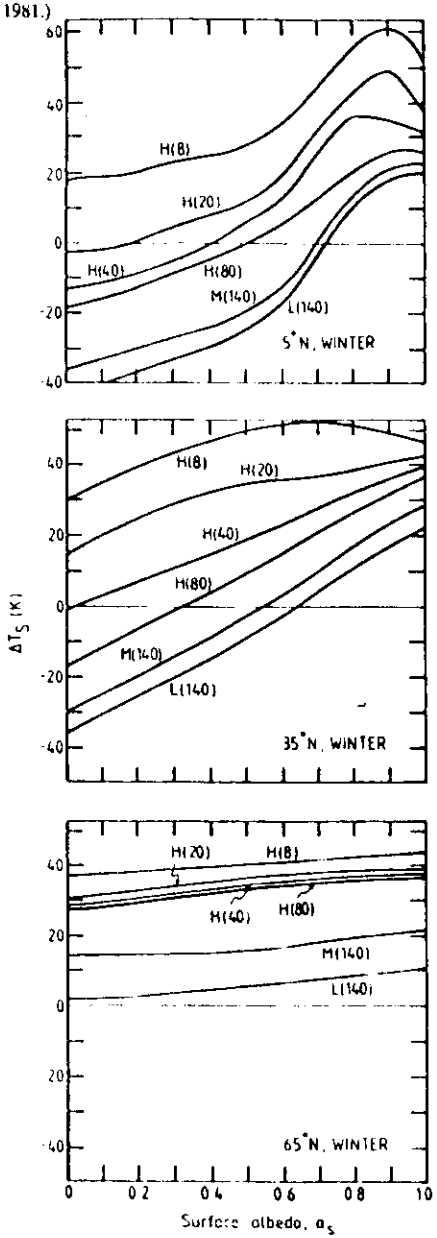

Fig. 3.3. Equilibrium surface temperature distributions as a function of cloud amount for three cloud layers using summer and winter solstice conditions at 35°N. Clouds are assumed to possess liquid water path values of 140, 140 and 20 gm^{-2} and occupy the layers 913-854, 632-549, and 381-301 mb respectively. (From Stephens and Webster, 1981.)

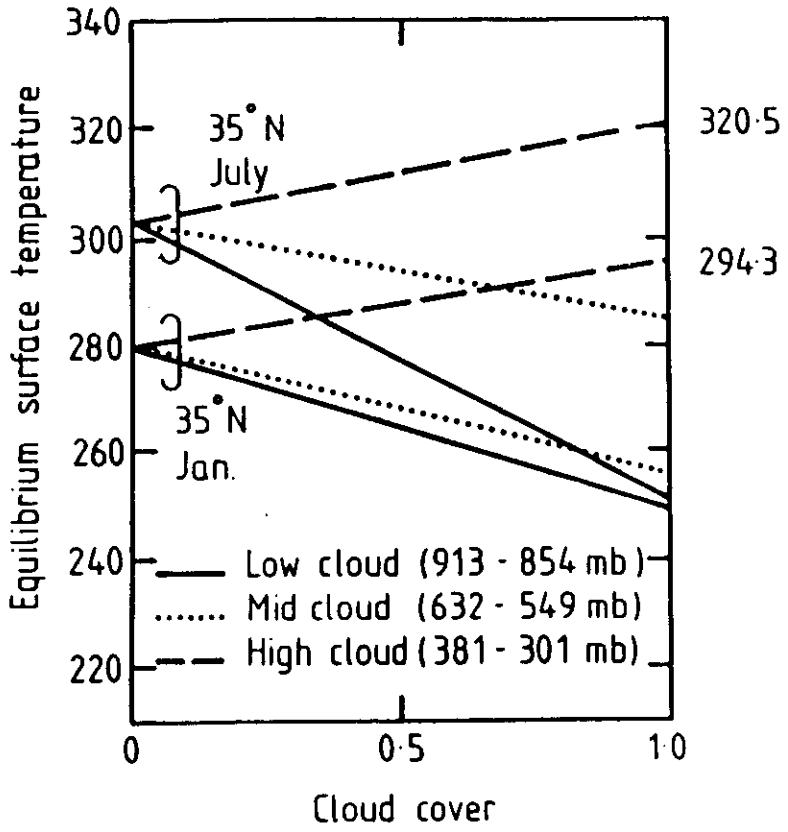

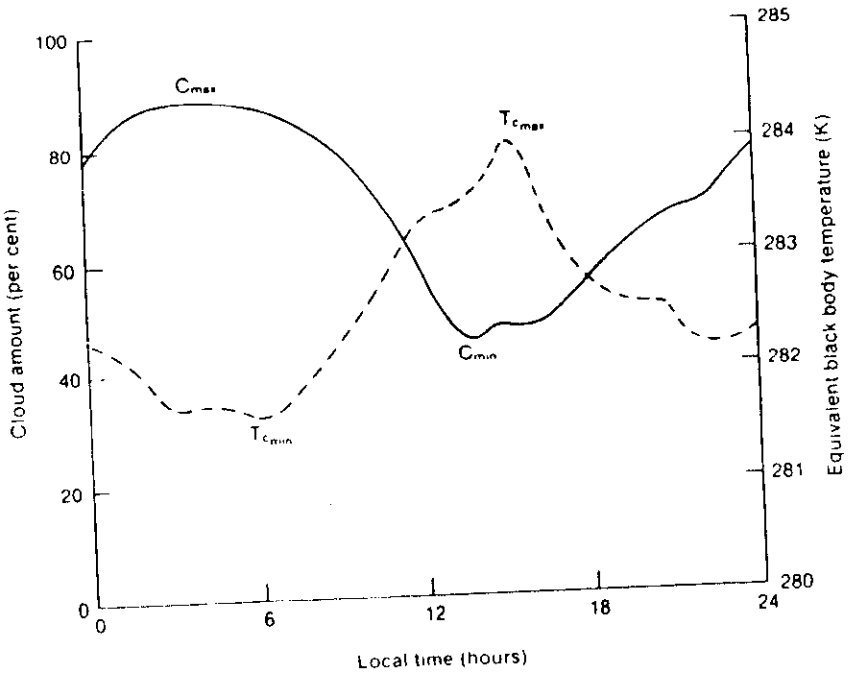

Fig. 4.1. Hourly average low cloud (<2 km) amount (----) and cloud top effective black-body temperature (- - -) in the eastern Pacific derived from GOES-E data during November 1978. (From Minnis and Harrison, 1984.)

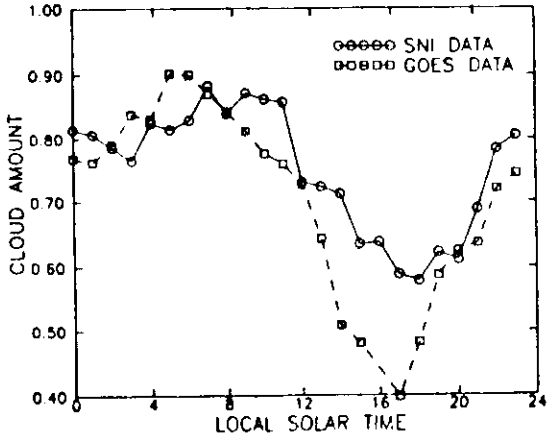

Fig. 4.2. Mean cloud amounts derived from GOES over a 0.5 ° × 1.0 ° region centered on San Nicolas Island and from island observations. (From Minnis et al, 1989.)

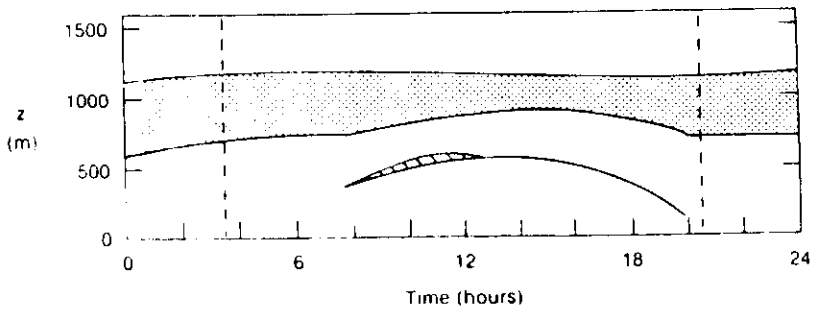

Fig. 4.3. Predicted diurnal variation of cloud layer. From integrations for mid-latitude stratocumulus in summer. (From Turton and Nicholls, 1987.)

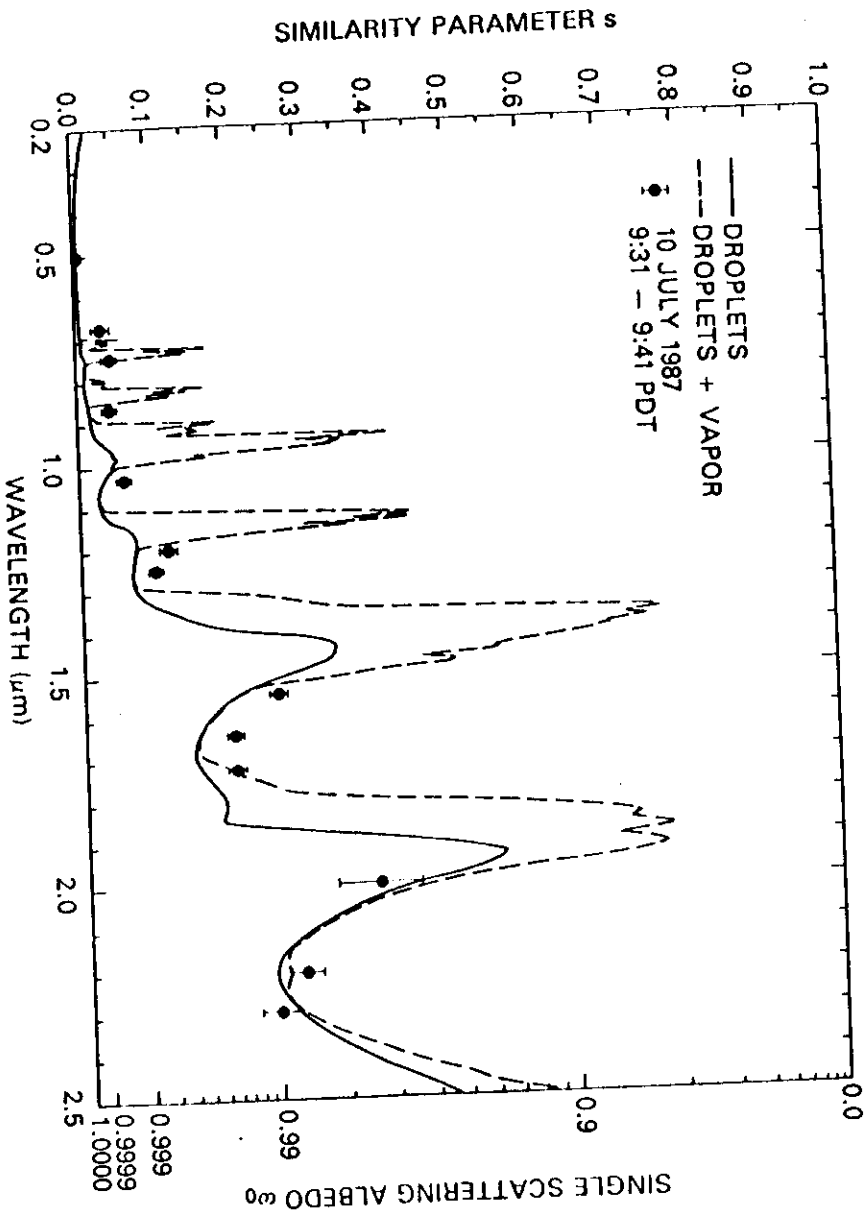

Fig. 4.4. Calculated and measured values of ω_0^2 with and without the contribution due to vapor. (From King et al., 1989.)

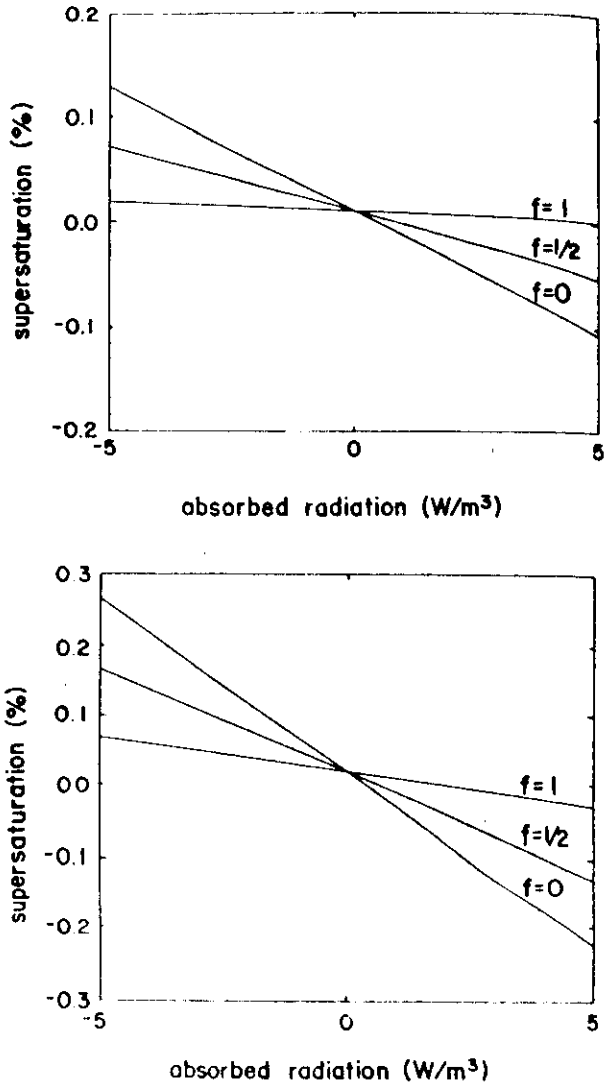

Fig. 4.5. Steady state supersaturation as a function of total absorbed radiation in the cloud for different values of f, the fraction of total radiation absorbed by the droplets: upper panel, nimbostratus cloud model; lower panel, stratocumulus cloud model. (From Davies, 1984.)